

# Supporting Information

## Enhanced toughness in highly entangled hydrogels via non-covalent molecular hooks

Élise Ansart,<sup>a</sup> Lucien Cousin<sup>a</sup>, Mark W. Tibbitt,<sup>a</sup> and Stefan Mommer<sup>\*,a</sup>

### Table of Contents

1	Experimental part .....	2
2	Tensile Testing .....	5
3	Gel Permeation Chromatography .....	4
4	NMR spectroscopy .....	7
5	References .....	9

---

<sup>a</sup> Macromolecular Engineering Laboratory, Department of Mechanical and Process Engineering, ETH Zurich, Sonneggstrasse 3, 8092, Zurich, CH. E-mail: [smommer@ethz.ch](mailto:smommer@ethz.ch)

# 1 Experimental part

## 1.1 Materials

Acrylamide (AAm, >99%, Sigma-Aldrich), 2,2'-azobis[2-(2-imidazolin-2-yl)propane]dihydrochloride (VA-044, >98%, TCI Chemicals) and poly(ethyleneglycol)dimethylether (PEGdme,  $M_n = 500$  g/mol, Sigma-Aldrich) were used without further purification. To remove the residual inhibitor, poly(ethyleneglycol)methyletheracrylate (PEGMeAc,  $M_n = 480$  g/mol, Sigma-Aldrich) and poly(ethyleneglycol)diacrylate (PEGDA,  $M_n = 500$ g/mol, Sigma-Aldrich) were first destabilized via a short column of basic alumina prior use. The acetate buffer was prepared at a concentration of 50 mM and the pH was adjusted to 4.75 using aqueous NaOH solution. Unless stated otherwise, all experiments were performed using ultrapure milli-Q water with a resistivity of  $18.2 \text{ M}\Omega \cdot \text{cm}^{-1}$  and all solvents were purchased from commercial sources and used without further modification.

## 1.2 Instrumentation

**$^1\text{H}$  NMR** spectra were recorded on a Bruker Biospin 400 NMR spectrometer (400 MHz) and are reported as follows: chemical shift  $\delta$  (ppm) (multiplicity, coupling constant  $J$  (Hz), number of protons, assignment). The residual protiated solvent signals of DMSO- $d_6$  ( $\delta_{\text{H}} = 2.50$  ppm) and D<sub>2</sub>O ( $\delta_{\text{H}} = 4.79$  ppm) were used as reference. Chemical shifts are reported in ppm to the nearest 0.01 ppm for  $^1\text{H}$ . The data was analyzed using the MestReNova software (Version 14.2.3-29241, Mestrelab Research S.L.).

**Gel Permeation Chromatography (GPC).** Molecular weights ( $M_n$  and  $M_w$ ) and dispersities ( $\text{Đ} = M_w/M_n$ ) were determined by size exclusion chromatography (SEC). SEC analyses were carried out on an OMNISEC Resolve system, equipped with an OMNISEC Reveal triple detector (refractive index, light scattering and viscosity). Milli-Q water was used as an eluent and contained 0.1 M of sodium nitrate and 0.02% (w/v) sodium azide, which was filtered through a 0.2  $\mu\text{m}$  Nylon filter before use. One guard column (8  $\times$  50 mm, AGuard, Viscotek) and two A6000M general mixed gel columns (8  $\times$  300 mm) were applied at a flow rate of  $0.7 \text{ mL} \cdot \text{min}^{-1}$  at 25 °C. The incremental refractive index value was set to  $dn/dc = 0.185$ , as previously reported for polyacrylamide in 0.1 M NaNO<sub>3</sub> phosphate buffer at pH = 8.<sup>[4]</sup> For sample preparation, polymerized samples were dissolved in the carrier phase at a concentration of  $1 \text{ mg} \cdot \text{mL}^{-1}$  for at least two days at ambient conditions. Each sample was injected at least twice and the values for  $M_n$ ,  $M_w$  and  $\text{Đ}$  were averaged accordingly. The determination of molecular weights was achieved through triple detection mode and the results were exported using the OMNISEC Software (Version 11.32, Malvern Panalytical).

**Rheology.** All mechanical characterization experiments were performed on the strain-controlled oscillatory Modular Compact Rheometer (MCR 502, Anton Paar) with a 20 mm diameter stainless steel (1.4404) parallel plate geometry (PP20, Anton Paar). The device was operated using the RheoCompass software (Anton Paar). The samples were loaded using disposable spatulas and excess material was trimmed at a gap distance of 1 mm. Samples were measured at a gap size of 1 mm and silicon oil was added at the outside rim of the tool to prevent the evaporation of water and drying of the samples. All measurements were performed at 25 °C. The characterization protocol included three phases, each subdivided into a preconditioning step and the actual measurement. For the preconditioning, both storage ( $G'$ ) and loss modulus ( $G''$ ) were recorded. Hereby, 24 data points were acquired in 120 s at a shear strain of  $\gamma = 0.5\%$  and an angular frequency of  $\omega = 1 \text{ rad}\cdot\text{s}^{-1}$ . During the actual measurements, six data points were recorded per decade using the parameter set described in the following. First, an oscillatory frequency sweep was performed by sweeping the angular frequency from 100 to 1  $\text{rad}\cdot\text{s}^{-1}$  at a constant shear strain of  $\gamma = 0.5\%$  and recording  $G'$  and  $G''$ . Next, the oscillatory amplitude sweep was carried out, varying the shear strain from 0.1 to 500% at  $\omega = 10 \text{ rad}\cdot\text{s}^{-1}$  angular frequency capturing  $G'$  and  $G''$ . Finally, the viscosity was measured in a steady-state shear rate sweep with shear rates ( $\dot{\gamma}$ ) ranging from 0.1 to 100  $\text{s}^{-1}$  at a 120 s timeout. For stress relaxation experiments, a shear strain of  $\gamma = 10\%$  was applied before sampling the relaxation modulus for 9.5 hours to reach equilibrium. Rotational shear experiments were carried out at a constant shear rate of 0.001  $\text{s}^{-1}$  to measure the shear stress values resulting from linearly increasing shear strain.

**Tensile testing.** Tensile testing experiments were performed on an Instron 5864 equipped with a 100 N load cell and hydraulic clamps. Cylindrical specimen were glued at each extremity within the hollow cylindrical cavity of 3D printed fixtures. The other side of the fixtures was a rigid straight bar to enable clamping to the apparatus. Specimen were stretched at a constant rate of 60 mm/min and true stress–strain curves were plotted using custom MATLAB code. Stiffness values were fitted between 0–10 % strain. Work of fracture was determined by measuring the area under the true stress–strain curve.

**Differential scanning calorimetry** (DSC) was performed on a Mettler Toledo 821<sup>e</sup> system under a nitrogen atmosphere (40 mL/min). The samples (~5 mg) were sealed and loaded in aluminum pans (100  $\mu\text{L}$ ), and an empty sample pan was used as the reference. Samples were scanned for three consecutive heating/cooling cycles within a temperature range of 25–300 °C and a heating rate of 10 °C/min. The first heating cycle erased the thermal history of the polymer and was therefore discarded, while the third heating cycle was used for the determination of the glass transition temperature ( $T_g$ ). The latter was determined by choosing the local maximum of the first derivative of the heating curve.

## 1.3 Synthesis

### 1.3.1 General procedure for the synthesis of UHMW (co)polymer hydrogels

AAM was dispersed in acetate buffer (2 M, pH = 4.75) at room temperature and VA-044 was added at 0 °C (0.005 mol% compared to AAm, from a 10 mg/mL solution in buffer). For copolymer samples, the desired amount of PEGmeAc (Mn = 480 g/mol, 1 or 5 mol%) was also added. The solution was briefly ultrasonicated on ice for homogenisation. The solution was subjected to 3 cycles of freeze-pump-thaw using liquid nitrogen to degas it. Finally, the reaction mixture was injected into commercially available NMR tubes previously flushed with Argon and polymerized at 70 °C for 4 h in an oil bath to give the hydrogel. The polymerized samples were screw-capped and stored at ambient conditions for at least one day prior to extraction of the cylindrical specimen by breaking the NMR tubes. A control sample was prepared by replacing PEGmeAc by PEGdme (Mn = 500g/mol). Samples were also prepared using PEDGA (Mn = 500 g/mol) as a covalent crosslinker or longer PEGmeAc groups (Mn = 1000 g/mol or 5000 g/mol).

Table S1. Experimental conditions for the synthesis of UHMW (co)polymer samples.

Compound	MW (g/mol)	Quantity (mol%) <sup>a</sup>	Gel stability
-	-	-	Flowing
PEGmeAc	480	1	Stable
PEGmeAc	480	5	Stable
PEGmeAc	1000	1	Flowing
PEGmeAc	5000	1	Viscous liquid
PEGDA	500	1	Stable
PEGdme	500	1	Flowing

<sup>a</sup> mol% values are related to the amount of AAm (2M in solution).

## 2 Gel Permeation Chromatography

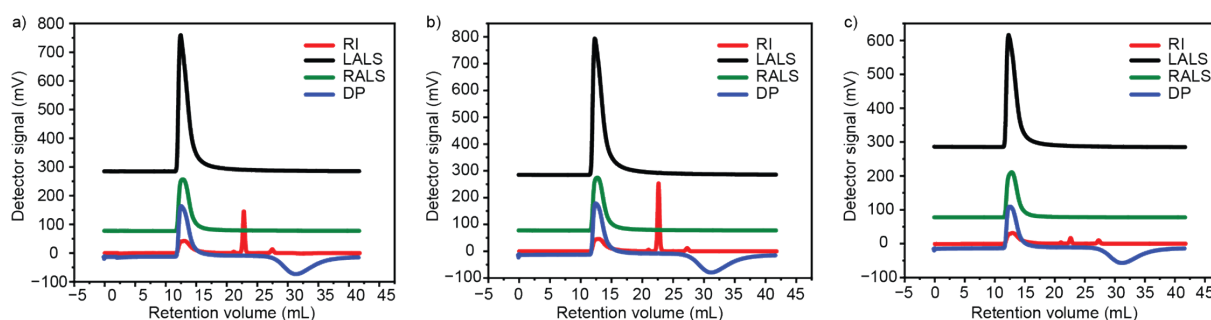


Figure S1. GPC analysis for three replicates of polyAAm chains synthesized from a 2M AAm solution with 0.005 mol% VA-044 in acetate buffer.  $M_n$  (MDa),  $M_w$  (MDa) and dispersity values were respectively equal to (3.5, 3.8, 1.1) for a), (3.6, 3.9, 1.1) for b) and (3.3, 3.6, 1.1) for c).

### 3 Tensile Testing

For the tensile tests, the gel precursor solution was loaded into a commercially available NMR tube as described in section 1.3.1. After being cured for 4 h at 70 °C, the sample had to be unmolded. For this the glass was pre-cut using a diamond cutter prior to slightly smashing it with a hammer to cause the glass to break. The shards were removed by use of a pair of tweezers to obtain the final cylindrical hydrogel specimen. The hydrogel specimen was then glued into a 3D printed fixture (Figure S2) using commercially available fast-drying contact glue. After this the sample specimen could be clamped to the upper clamp of the tensile tester. By lowering the sample gradually, the other end of the hydrogel could be connected (also by using glue) with the lower 3D printed fixture, which had already been attached to the lower clamp of the tensile tester. Once the hydrogel was fixated and in place, the tensile measurement could be started.

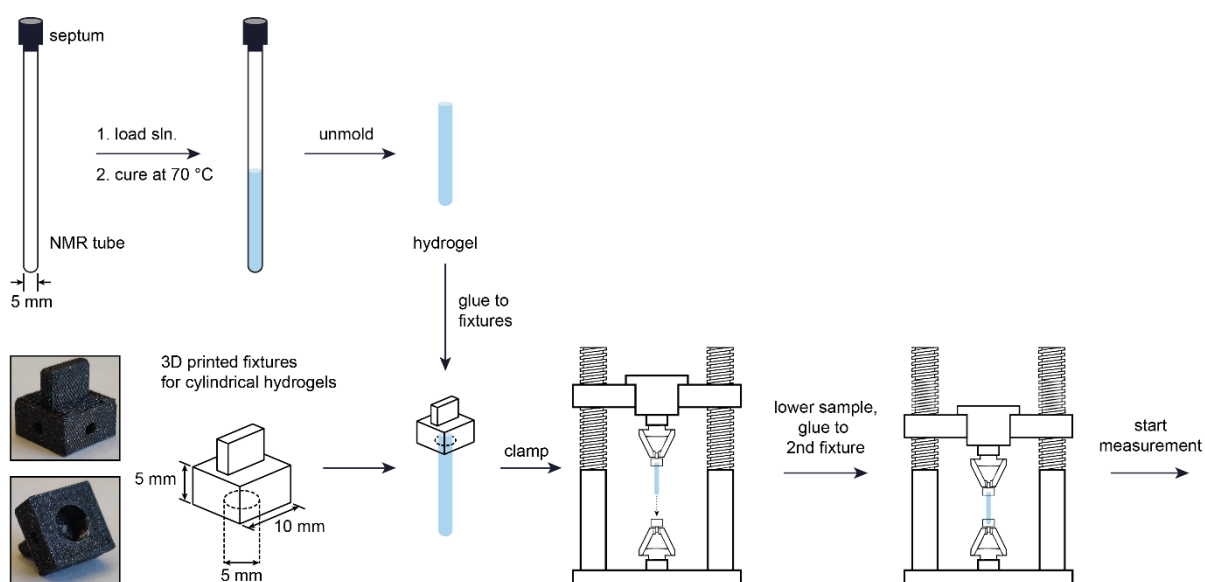


Figure S2. Schematic procedure to prepare cylindrical hydrogels for the tensile measurements using custom-designed 3D-printed fixtures.

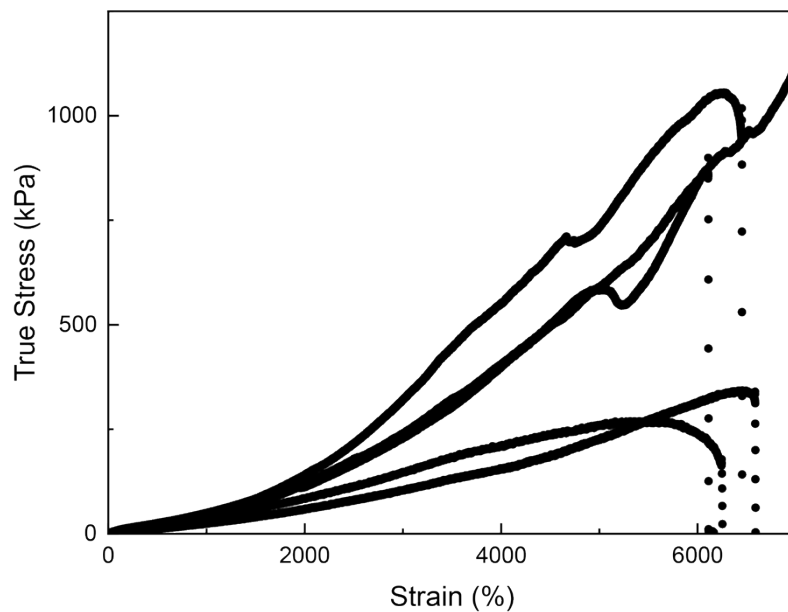


Figure S3. True stress–strain curves of copolymer samples (1 mol% PEGmeAc) from different polymerization batches. Two outliers showed deviating data, which was likely caused through small fissured and defects introduced to the sample upon unmolding.

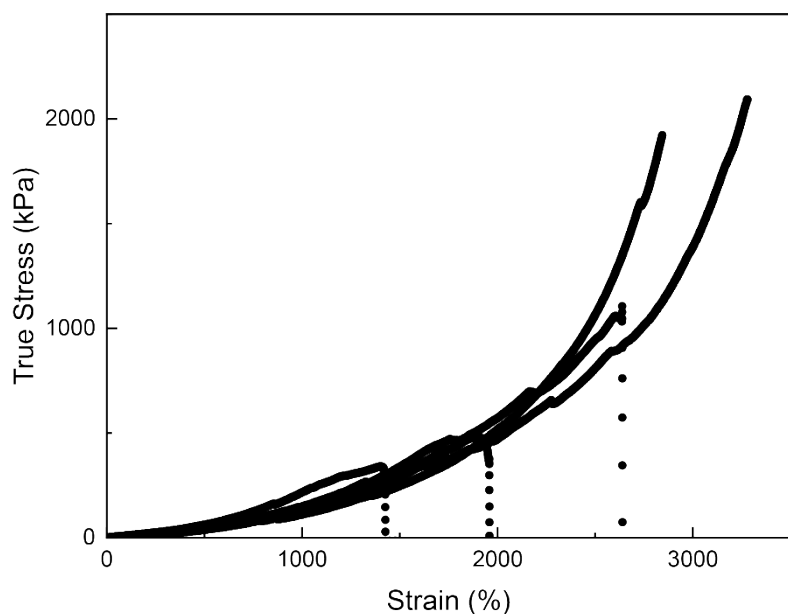


Figure S4. True stress–strain curves of copolymer samples (5 mol% PEGmeAc) from different polymerization batches. Two outliers showed deviating data which was likely caused through small fissured and defects introduced to the sample upon unmolding.

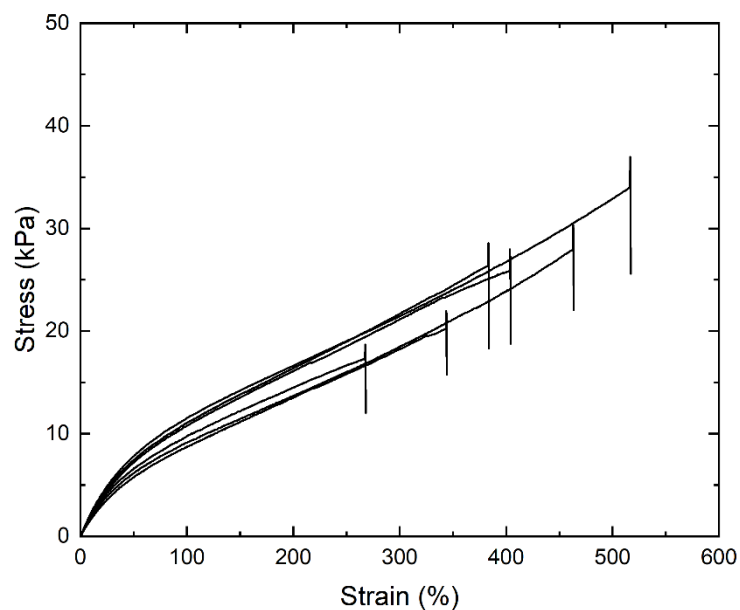


Figure S5. True stress–strain curves of various control samples with high entanglements but no PEGmeAc side chains (0.05 mol% PEGDA).

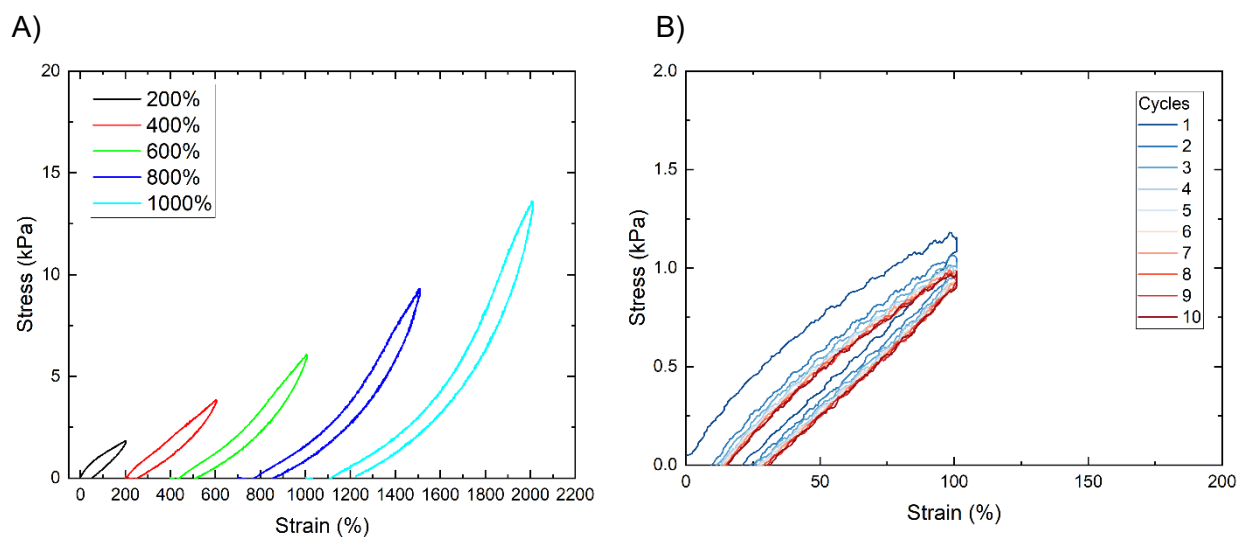


Figure S6. Cyclic tensile tests of poly(AAm-*stat*-PEGmeAc) using 1 mol% PEGmeAc by applying A) strain amplitudes of 200, 400, 600, 800 and 1000% successively and B) stretching the sample to 100% for 10 cycles in a row without relaxation time.

## 4 Rheology

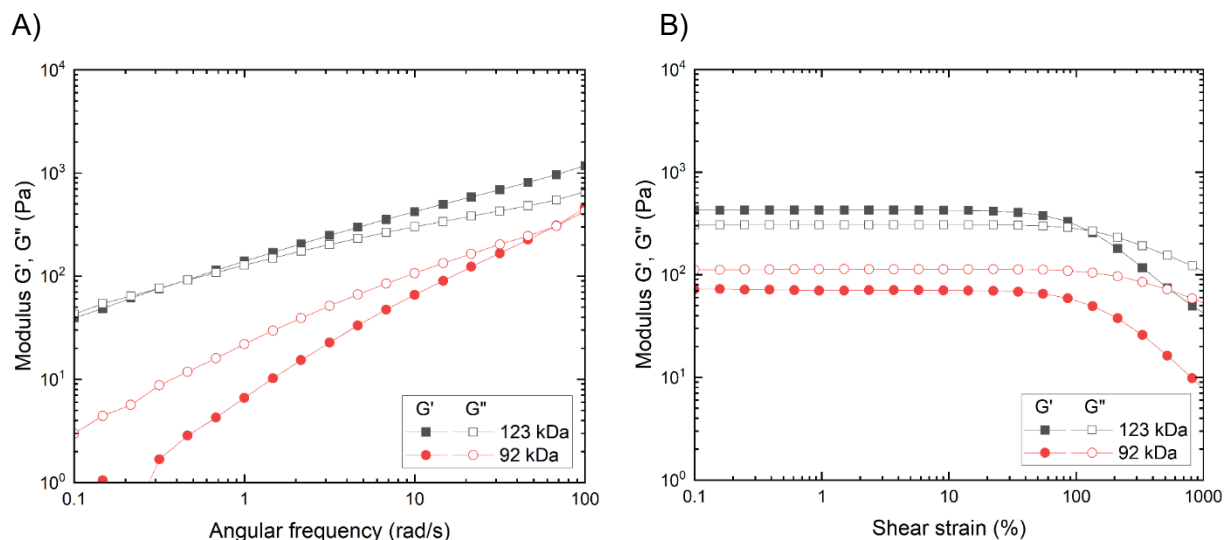


Figure S7. A) Frequency sweeps ( $\omega = 100\text{--}0.1 \text{ rad}\cdot\text{s}^{-1}$ ,  $\gamma = 0.5\%$ ) and B) strain sweeps ( $\gamma = 0.1\text{--}1000\%$ ,  $\omega = 10 \text{ rad}\cdot\text{s}^{-1}$ ) of polymer hydrogels with few entanglements by using 1 mol% of initiator VA-044, achieving molecular weights of 123 kDa and 92 kDa, respectively. Storage and loss moduli are depicted as filled and hollow symbols, respectively.

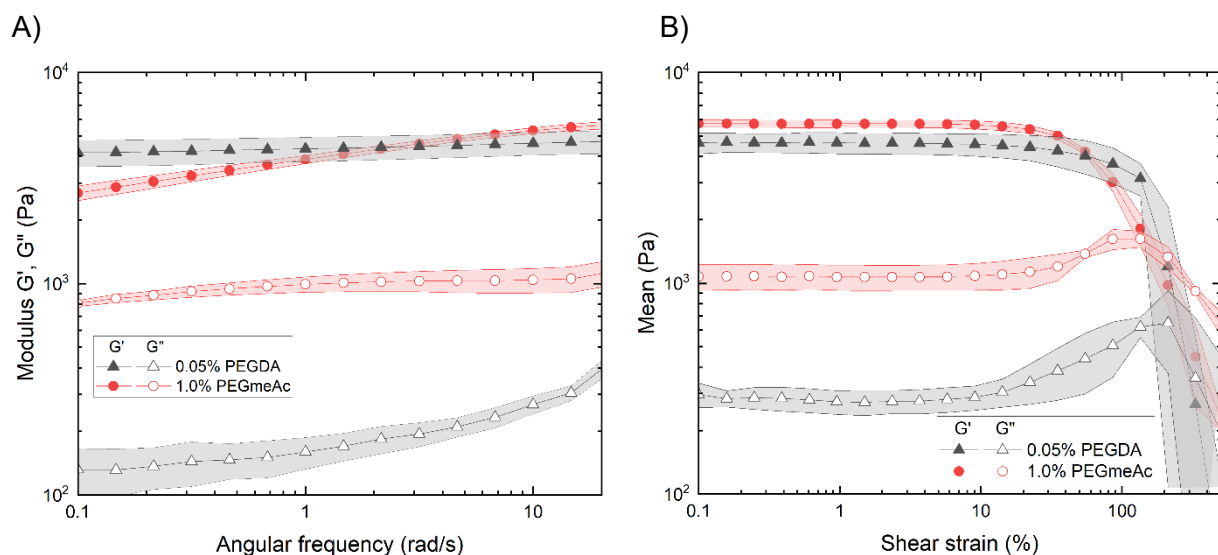


Figure S8. A) Frequency sweeps ( $\omega = 20\text{--}0.1 \text{ rad}\cdot\text{s}^{-1}$ ,  $\gamma = 0.5\%$ ) and B) strain sweeps ( $\gamma = 0.1\text{--}1000\%$ ,  $\omega = 10 \text{ rad}\cdot\text{s}^{-1}$ ) of covalent polymer hydrogels with high entanglements by using 0.05 mol% PEGDA and 0.005 mol% of initiator VA-044. The plots show mean values of storage and loss moduli as filled and hollow symbols as well as standard deviation ( $n = 3$ ) as shaded areas.



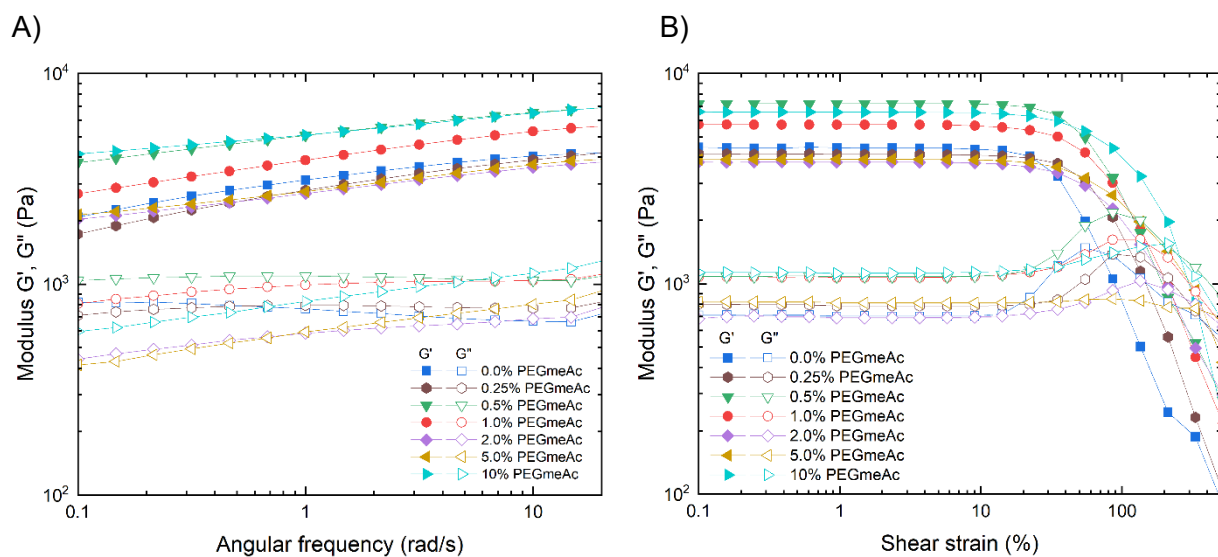


Figure S9. A) Frequency sweeps ( $\omega = 20\text{--}0.1 \text{ rad}\cdot\text{s}^{-1}$ ,  $\gamma = 0.5\%$ ) and B) strain sweeps ( $\gamma = 0.1\text{--}500\%$ ,  $\omega = 10 \text{ rad}\cdot\text{s}^{-1}$ ) of polymer hydrogels with 0.0 mol% (blue), 0.25 mol% (brown), 0.5 mol% (green), 1.0 mol% (red), 2.0 mol% (purple), 5.0 mol% (gold) and 10 mol% (cyan) of PEGmeAc. Storage and loss moduli are depicted as filled and hollow symbols, respectively.

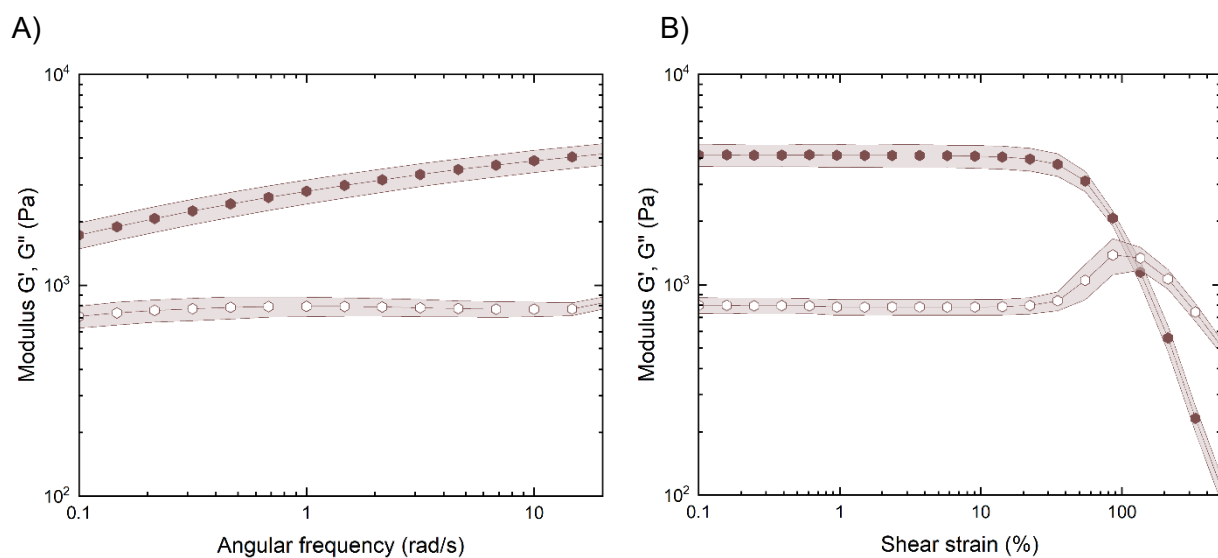


Figure S10. A) Frequency sweep ( $\omega = 20\text{--}0.1 \text{ rad}\cdot\text{s}^{-1}$ ,  $\gamma = 0.5\%$ ) and B) strain sweep ( $\gamma = 0.1\text{--}500\%$ ,  $\omega = 10 \text{ rad}\cdot\text{s}^{-1}$ ) of polymer hydrogels with 0.25 mol% of PEGmeAc. The plots show mean values of storage and loss moduli as filled and hollow symbols as well as standard deviation ( $n = 3$ ) as shaded areas.

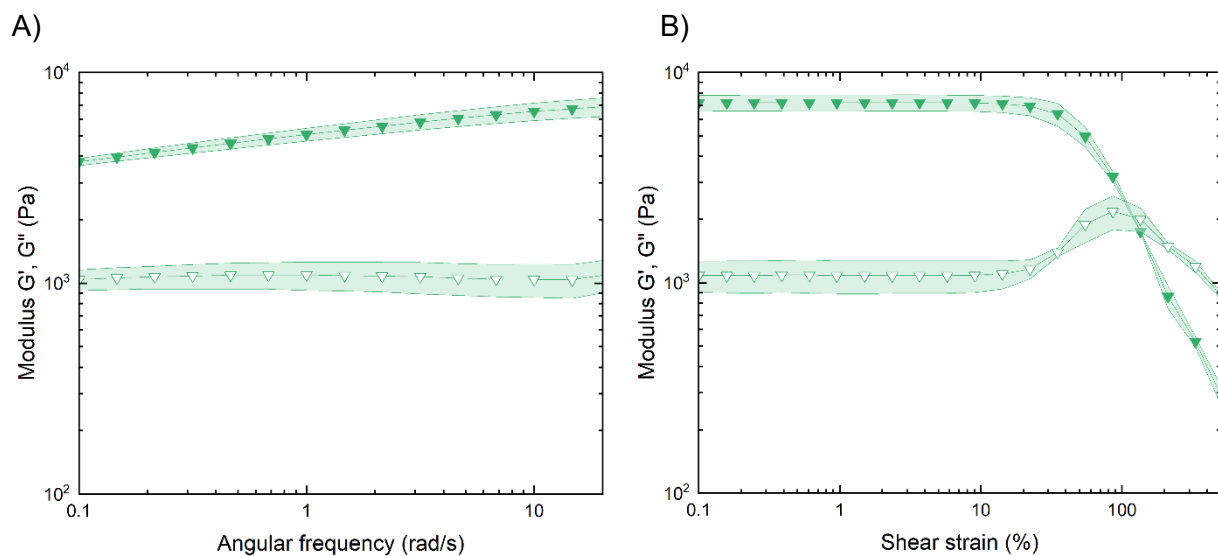


Figure S11. A) Frequency sweep ( $\omega = 20\text{--}0.1 \text{ rad}\cdot\text{s}^{-1}$ ,  $\gamma = 0.5\%$ ) and B) strain sweep ( $\gamma = 0.1\text{--}500\%$ ,  $\omega = 10 \text{ rad}\cdot\text{s}^{-1}$ ) of polymer hydrogels with 0.5 mol% of PEGmeAc. The plots show mean values of storage and loss moduli as filled and hollow symbols as well as standard deviation ( $n = 3$ ) as shaded areas.

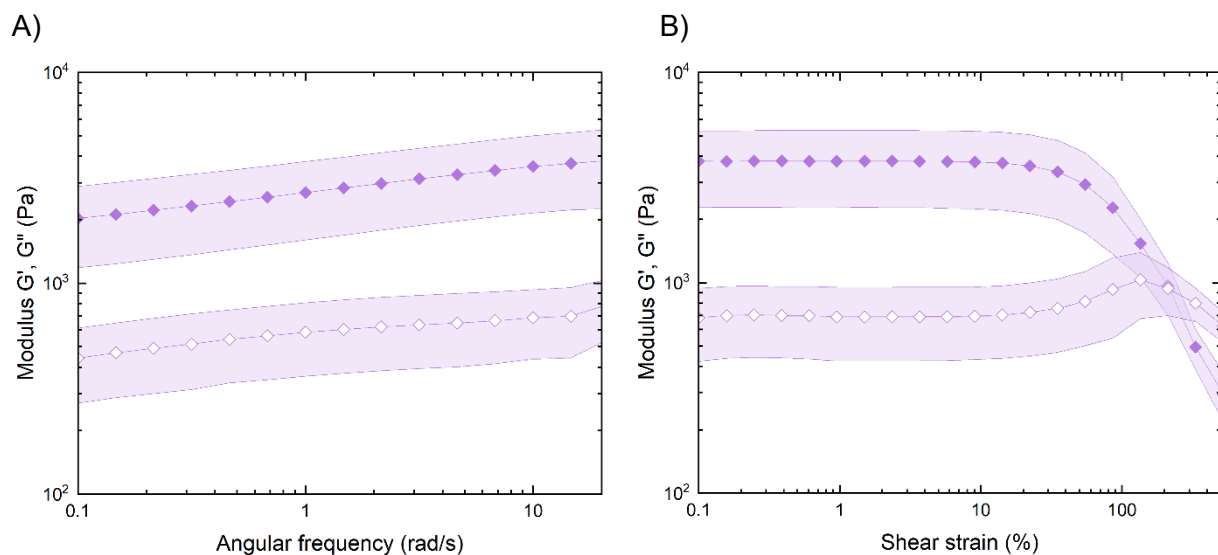


Figure S12. A) Frequency sweep ( $\omega = 20\text{--}0.1 \text{ rad}\cdot\text{s}^{-1}$ ,  $\gamma = 0.5\%$ ) and B) strain sweep ( $\gamma = 0.1\text{--}500\%$ ,  $\omega = 10 \text{ rad}\cdot\text{s}^{-1}$ ) of polymer hydrogels with 2.0 mol% of PEGmeAc. The plots show mean values of storage and loss moduli as filled and hollow symbols as well as standard deviation ( $n = 3$ ) as shaded areas.

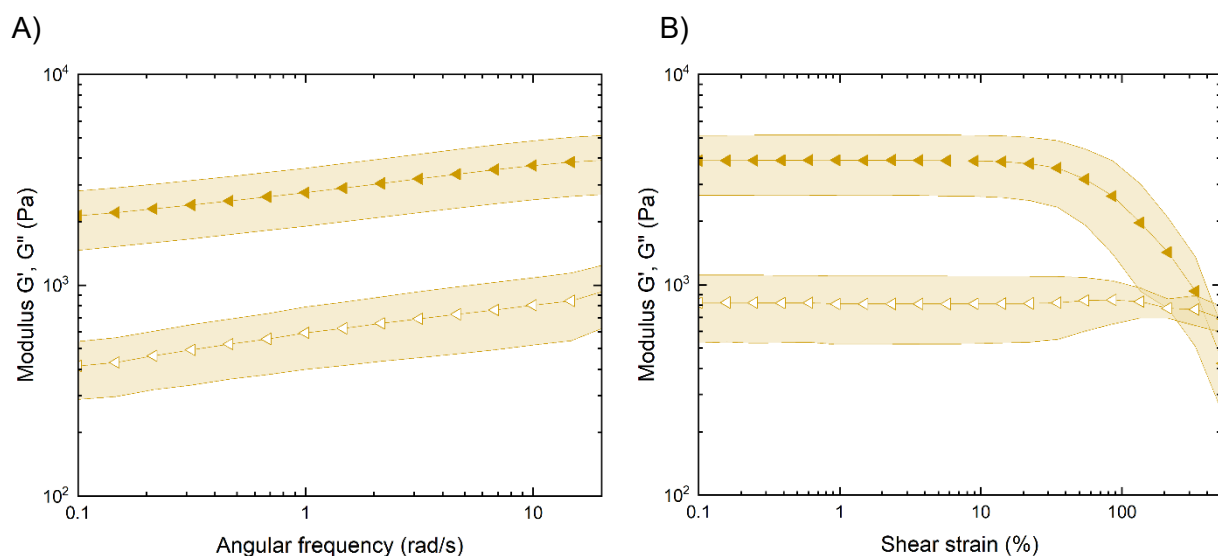


Figure S13. A) Frequency sweep ( $\omega = 20\text{--}0.1 \text{ rad}\cdot\text{s}^{-1}$ ,  $\gamma = 0.5\%$ ) and B) strain sweep ( $\gamma = 0.1\text{--}500\%$ ,  $\omega = 10 \text{ rad}\cdot\text{s}^{-1}$ ) of polymer hydrogels with 5.0 mol% of PEGmeAc. The plots show mean values of storage and loss moduli as filled and hollow symbols as well as standard deviation ( $n = 3$ ) as shaded areas.

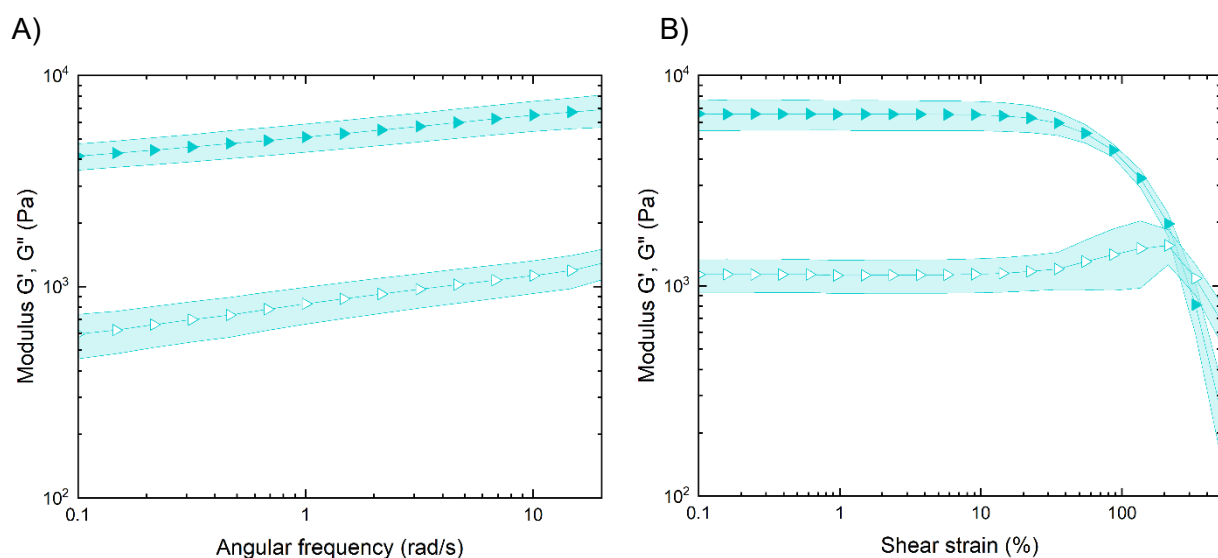


Figure S14. A) Frequency sweep ( $\omega = 20\text{--}0.1 \text{ rad}\cdot\text{s}^{-1}$ ,  $\gamma = 0.5\%$ ) and B) strain sweep ( $\gamma = 0.1\text{--}500\%$ ,  $\omega = 10 \text{ rad}\cdot\text{s}^{-1}$ ) of polymer hydrogels with 10 mol% of PEGmeAc. The plots show mean values of storage and loss moduli as filled and hollow symbols as well as standard deviation ( $n = 3$ ) as shaded areas.

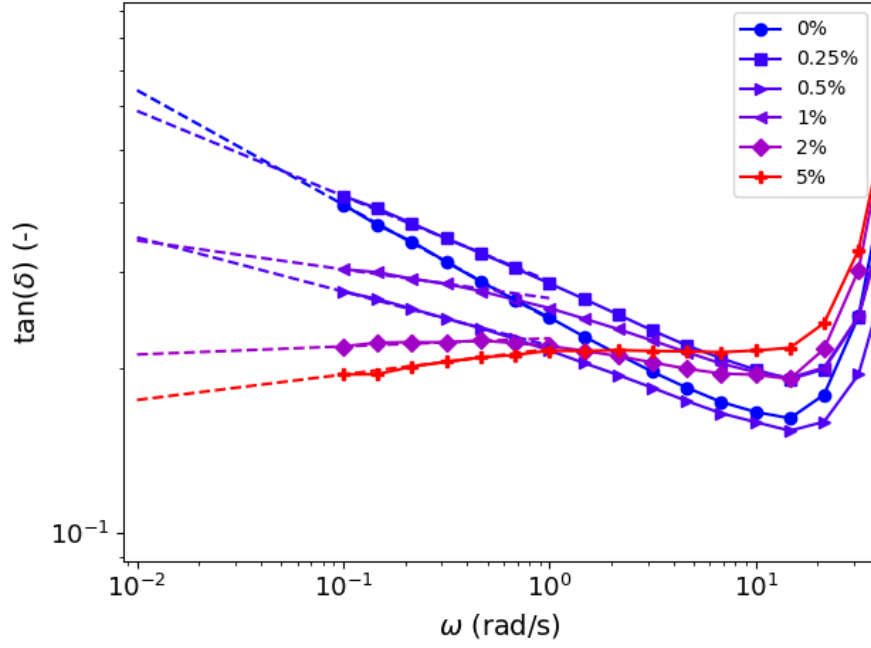


Figure S15. Loss factor ( $\tan \delta$ ) of polymer hydrogels with 0.0 mol%, 0.25 mol%, 0.5 mol%, 1.0 mol%, 2.0 mol%, and 5.0 mol% of PEGmeAc. The lowest four frequencies were fitted to a simple power law and the linear regression was extrapolated to  $\tan \delta = 1$  to estimate the relaxation time  $\tau_R$ .

Table S2. Estimated relaxation times of hydrogels with different concentrations of PEGmeAc through extrapolation of  $\tan \delta$ . Relaxation times above 1.0 mol% approached infinity.

PEGmeAc [mol%]	$\tau_R$ [s]
0.0	$8.28\text{E}2 \pm 29$
0.25	$2.85\text{E}3 \pm 1.35\text{E}3$
0.50	$4.32\text{E}6 \pm 1.48\text{E}6$
1.0	$3.69\text{E}9 \pm 9.59\text{E}8$

#### Use of the Eyring equation:

Using the Eyring equation, we can write

$$\tau_R \propto T^{-1} \cdot e^{\frac{\Delta G}{kT}}$$

where  $T$  is the absolute temperature,  $k$  is the Boltzmann constant, and  $\Delta G$  is the energetic barrier associated with bond detachment. If our hypothesis is valid, then  $\Delta G$  should scale linearly with PEGmeAc concentration. To verify this,  $\log \tau_R$  was plotted vs. PEGmeAc concentration, where the PEGmeAc concentration is taken as mol% of PEGmeAc (Figure 3c). Noticeably, all points collapsed on the same line and assuming the bond detachment is mostly enthalpic (hydrogen bonding), an enthalpy for bond detachment per mol% PEGmeAc can be calculated amounting to 128 kJ/mol.

To further show that this energy corresponds to the activation energy of the bonds formed between PEGmeAc and PAAm, we measured  $\tau_R$  for a gel with 1 mol% PEGmeAc at temperatures ranging from 5 to 50 °C:

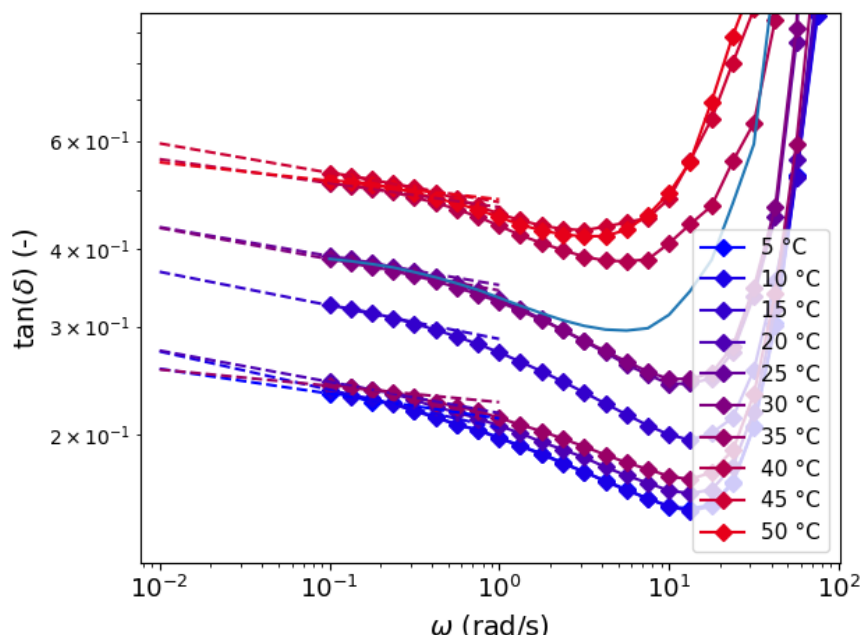


Figure S16. Loss factor ( $\tan \delta$ ) of polymer hydrogels with 1.0 mol% PEGmeAc, measured at various temperatures ranging from 5–50 °C. The lowest four frequencies were fitted to a simple power law and the linear regression was extrapolated to  $\tan \delta = 1$  to estimate the relaxation time  $\tau_R$ .

Using the Eyring equation, one can then plot  $\log(\tau_R \cdot T)$  versus  $1/T$ :

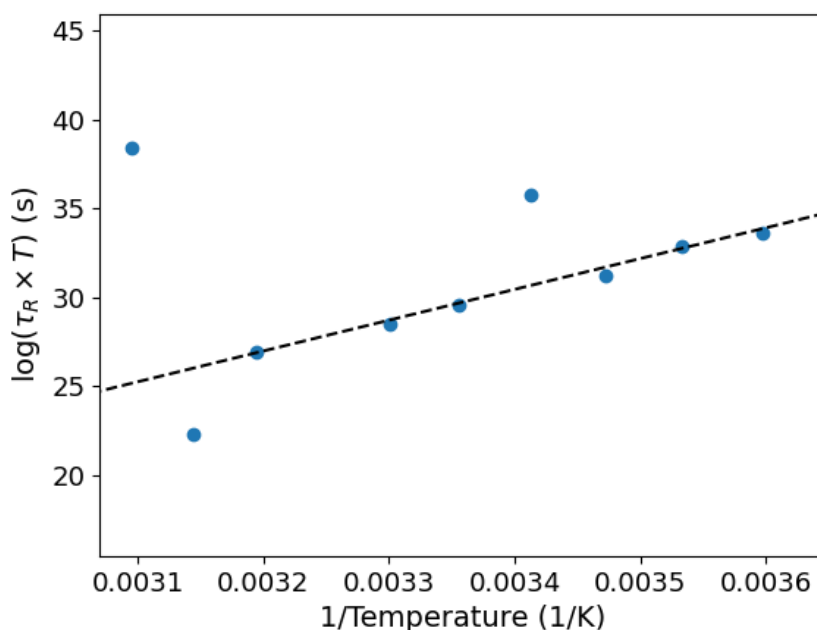


Figure S17. Eyring plot of a gel with 1 mol% PEGmeAc showing the logarithmic estimated relaxation time vs. the inverse of the absolute temperature. Experimental data points (blue spheres) are fitted with an affine function  $f(T) = 17350 \cdot 1/T - 28.56$  (dashed line).

If the bond detachment rate follows the Eyring equation, the resulting plot is a line with slope  $\Delta H/R$ , where  $\Delta H$  is the enthalpy of activation. Again it is indeed observed that all points collapse on a line, and  $\Delta H = 144 \text{ kJ/mol}$  is measured, which is in reasonable agreement with the value found varying the PEGmeAc concentration.

Together, these findings suggest that the introduction of PEGmeAc chains creates additional interactions associated with an energy barrier for the motion and disentanglements of the pAAm chains. We were able to measure this energy of activation and showed that it is proportional to the density of PEGmeAc chains.

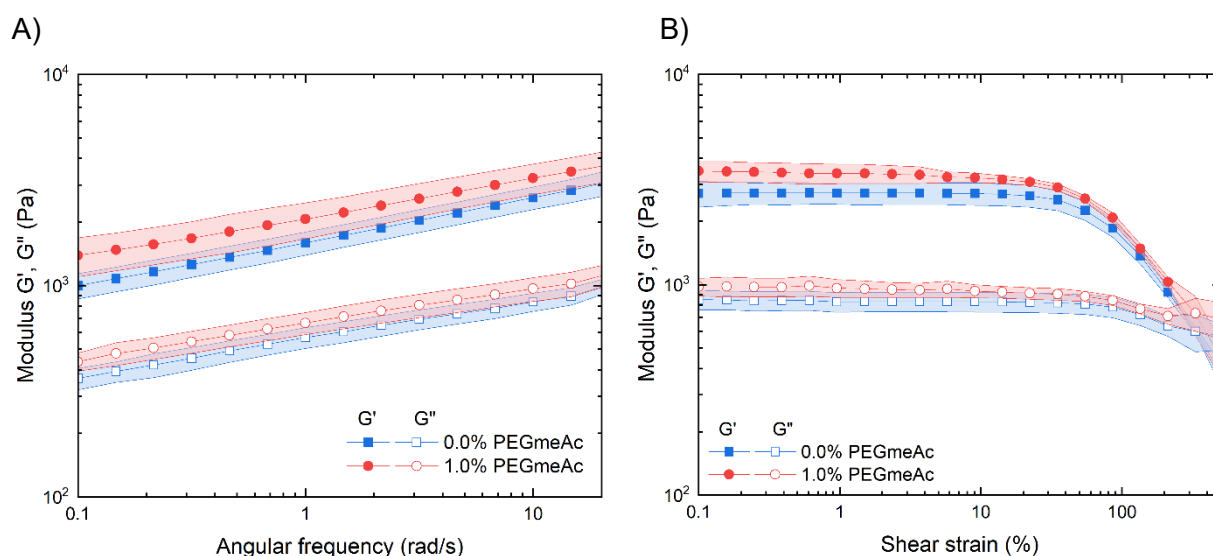


Figure S18. A) Frequency sweep ( $\omega = 20-0.1 \text{ rad}\cdot\text{s}^{-1}$ ,  $\gamma = 0.5\%$ ) and B) strain sweep ( $\gamma = 0.1-500\%$ ,  $\omega = 10 \text{ rad}\cdot\text{s}^{-1}$ ) of hydroxyethyl acrylamide hydrogels with 0 mol% (blue) and 1 mol% of PEGmeAc. The plots show mean values of storage and loss moduli as filled and hollow symbols as well as standard deviation ( $n = 3$ ) as shaded areas.

## 5 Differential scanning calorimetry

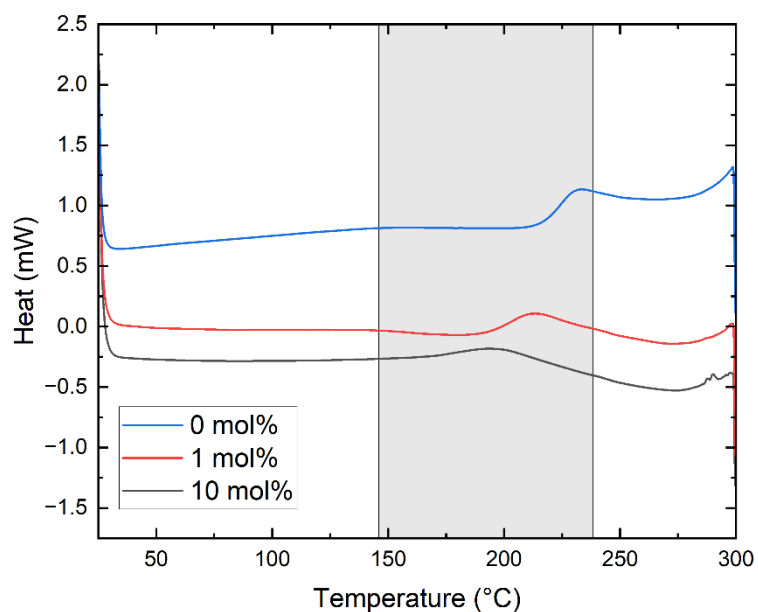


Figure S19. DSC thermograms of polyAAm, copolymerized with 0 mol% (blue), 1 mol% (red) and 10 mol% (black) of PEGmeAc, measured in a temperature range of  $T = 25\text{--}300\text{ }^{\circ}\text{C}$  using a standard heating rate of  $10\text{ }^{\circ}\text{C}/\text{min}$ . The gray shaded area was used to calculate the first derivative for the estimation of  $T_g$  in Figure S15.

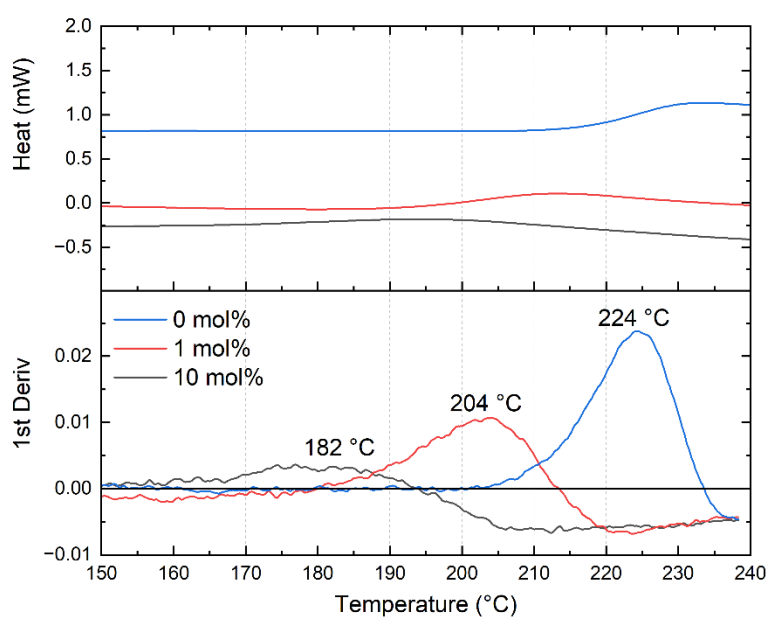


Figure S20. Magnification of the DSC thermograms of polyAAm, copolymerized with 0 mol% (blue), 1 mol% (red) and 10 mol% (black) of PEGmeAc (top) and the respective first derivatives to estimate the glass transition temperatures (bottom).

## 6 NMR spectroscopy

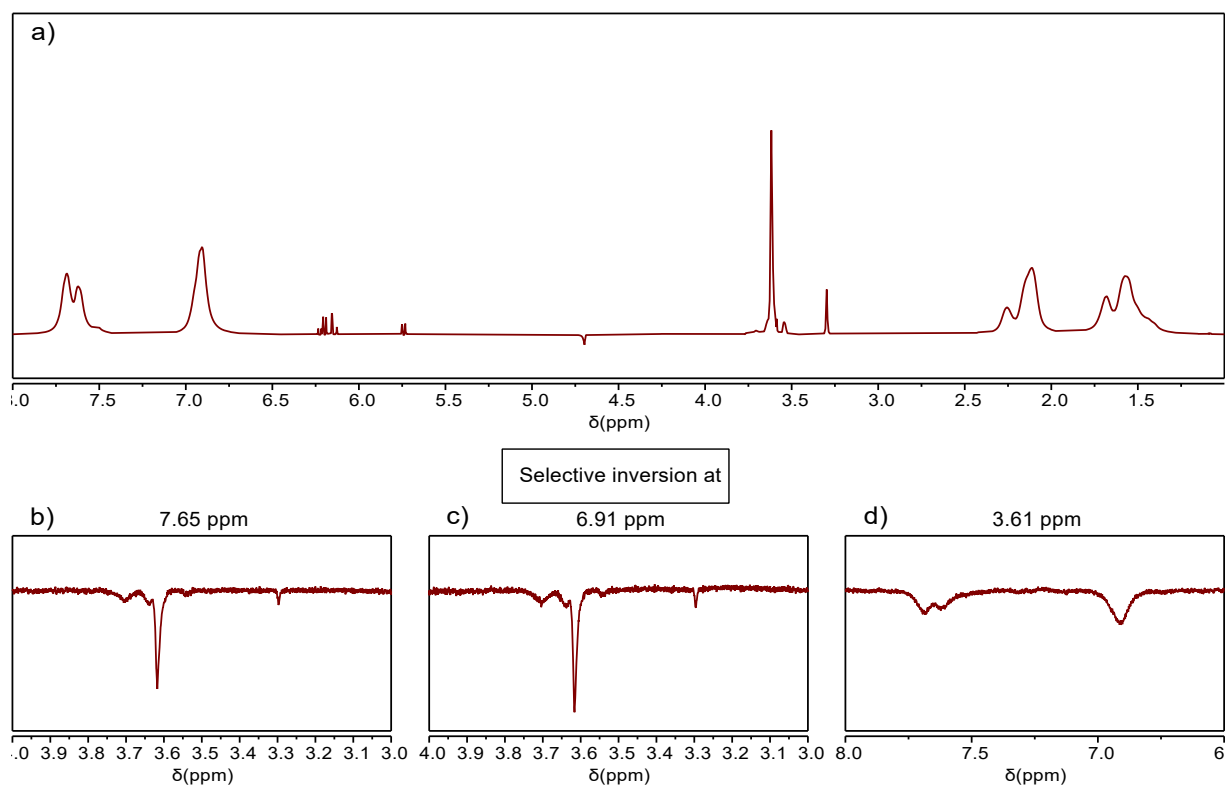


Figure S21. a)  $^1\text{H}$  NMR spectrum with excitation sculpting of poly(AAm-*stat*-PEGmeAc) in a  $\text{H}_2\text{O}$ - $\text{D}_2\text{O}$  mixture (95:5).  $^1\text{H}$  NOE signals of poly(AAm-*stat*-PEGmeAc) when selectively inverted at b) 7.65 ppm, c) 6.91 ppm, and d) 3.61 ppm. Number of scans = 1024, mixing time  $d_8 = 0.10$  s.



## 7 References

- [1] a) S. Keller, C. Vargas, H. Zhao, G. Piszczek, C. A. Brautigam, P. Schuck, *Anal. Chem.* **2012**, *84*, 5066-5073; b) T. H. Scheuermann, C. A. Brautigam, *Methods* **2015**, *76*, 87-98.
- [2] C. A. Brautigam, H. Zhao, C. Vargas, S. Keller, P. Schuck, *Nat. Protoc.* **2016**, *11*, 882-894.
- [3] C. A. Brautigam, in *Methods Enzymol.*, Vol. 562 (Ed.: J. L. Cole), Academic Press, **2015**, pp. 109-133.
- [4] A. Mejia, L. Rodriguez, C. Schmitt, N. Andreu, C. Favéro, O. Braun, G. Dupuis, E. Deniau, S. Reynaud, B. Grassl, *ACS Omega* **2019**, *4*, 11119-11125.
- [5] D. A. Kurgachev, O. A. Kotelnikov, D. V. Novikov, V. R. Kusherbaeva, S. I. Gorbin, E. V. Tomilova, A. Zhaksynbaeva, N. B. Dementeva, V. S. Malkov, A. A. Bakibaev, *Chromatographia* **2018**, *81*, 1431-1437.
- [6] a) J. Kim, I.-S. Jung, S.-Y. Kim, E. Lee, J.-K. Kang, S. Sakamoto, K. Yamaguchi, K. Kim, *J. Am. Chem. Soc.* **2000**, *122*, 540-541; b) A. Day, A. P. Arnold, R. J. Blanch, B. Snushall, *J. Org. Chem.* **2001**, *66*, 8094-8100.
- [7] S. Liu, C. Ruspic, P. Mukhopadhyay, S. Chakrabarti, P. Y. Zavalij, L. Isaacs, *J. Am. Chem. Soc.* **2005**, *127*, 15959-15967.
- [8] W. L. Mock, N. Y. Shih, *J. Org. Chem.* **1986**, *51*, 4440-4446.